On the tribological characterization of novel SiNb and SiW cast irons

Ş. Hakan Atapek[*,1], Gülşah Aktaş Çelik[1], Abdulaziz Alkan[1], İrem Altın[1], Şeyda Polat[1], Eleni Kamoutsi[2], Gregory Haidemenopoulos[2]
Kocaeli University, Department of Metallurgical and Materials Engineering, Laboratory of High Temperature Materials, Kocaeli-Türkiye[1]
University of Thessaly, Department of Mechanical Engineering, Laboratory of Materials, Volos-Greece[2]
*hatapek@kocaeli.edu.tr

Abstract: *In this study, the tribological behavior of new generation cast irons (SiNb and SiW) developed as an alternative to cast irons containing high silicon and molybdenum (SiMo) is investigated under dry friction conditions. All cast irons are produced by sand mold casting as Y blocks according to ASTM A536-84 standard and metallurgical characterization studies have revealed that they all have spheroidal graphite and dispersed carbides like Mo-rich M_6C, Nb-rich MC and W-rich M_6C type depending on the alloying element, within a ferritic matrix. Although no significant change is observed in the spherical morphology of graphite in cast iron matrices, a significant change is observed in the amount of graphite and image analysis studies reveal that the graphite content (area-%) in SiNb and SiW cast irons is 4,02 and 4,30, respectively, compared to SiMo cast iron (5,80). A significant change in the hardness of cast irons is also determined depending on the microstructural features; SiNb (228 ± 7 HV10) and SiW (218 ± 5 HV10) cast irons have higher hardness values compared to SiMo cast iron (192 ± 5 HV10). Cast irons and alumina ball as counterpart material are subjected to a tribological interaction for 150 m under dry friction conditions at a nominal load of 10 N and a ball sliding speed of 0.08 m/s and the findings indicate that (i) the coefficient of friction (CoF) decreases as the graphite content increases, with SiMo having the lowest CoF (0.023), followed by SiW (0.025), and SiNb showing the highest CoF (0.040), (ii) the specific wear rate increases as the hardness decreases, therefore, SiMo has the highest specific wear rate, whereas SiNb demonstrates the lowest specific wear rate and (iii) adhesive wear is the dominant wear mechanism for all ductile cast irons due to the presence of their ferritic matrix.*

Keywords*: CAST IRON, MICROSTRUCTURE, TRIBOLOGY, CHARACTERIZATION*

1. Introduction

Nodular graphite cast irons are materials with high tensile strength, high plastic deformation ability and fatigue resistance, and with these properties they are preferably used in many industrial applications, like the automotive industry [1], especially in engine blocks, exhaust manifolds, gearboxes, turbocharger/pump components [2, 3]. It is a fact that the automotive industry needs to take many precautions (i.e. reduced CO_2 emissions) in accordance with the environmental regulations. However, it is inevitable that the systems aim to operate at higher temperatures and thus increase fuel efficiency and compression ratio [4, 5]. This brings the need for materials with high metallurgical/mechanical stability that are resistant to oxidation/corrosion, especially at higher temperatures, for engine components. Although these properties are largely achieved by stainless steels and nickel-based materials, spheroidal graphite cast irons come to the fore commercially as the mostly used materials due to their low costs [3, 6, 7].

Among spheroidal graphite cast irons, SiMo cast irons are the most widely used materials for engine components. During the production of cast iron, the effect of inoculants on graphitization tendency and high nodularity graphite formation is undeniable [8-10]. Graphitization of SiMo cast iron is promoted due to the presence of silicon in the chemical composition, and at the same time a ferritic matrix is obtained [11]. With silicon, the austenite transformation temperature can be shifted, and thus microstructural and mechanical stabilization can be achieved at higher temperatures. Although the yield strength increases due to the increase in the amount of silicon, toughness and elongation (%) decrease [12]. The matrix structure of this type of cast iron is essentially ferritic, and pearlite, graphite and Mo-rich carbides (M_6C) can also be found embedded in the matrix [13]. On the other hand, with the contribution of molybdenum, a significant increase in the high-temperature properties of this cast iron can be achieved. It is also possible to increase the oxidation resistance, creep resistance and high temperature wear resistance of SiMo cast iron by increasing its molybdenum content. It is inevitable that molybdenum will be segregated to the cell boundaries in solidification and thus boundary carbides will be formed. Although these carbides increase tensile strength, creep and corrosion resistance, they significantly reduce the plasticity of the material [6, 14, 15].

In recent years, an intense effort has been made to further improve the high temperature properties of SiMo cast iron on one hand and mechanical properties on the other. While many studies focus on the modification of SiMo cast iron with elements such as Al and Cr, some studies focus on the development of new generation cast irons using thermodynamic approaches. Among the new generation cast irons, SiNb-*x*Al and SiW-*x*Al, having 0-4% Al by weight, are noteworthy. Compared to SiMo cast irons, the aforementioned cast irons have a higher A_1 temperature and higher oxidation resistance. Considering the mechanical properties of these materials, it is possible that elements such as Nb and W contribute to the formation of hard carbides and that the ferrite phase is hardened with the addition of aluminum [13, 14, 16, 17].

In this study, the tribological characterization of the new generation cast irons, which offer an advantage compared to SiMo cast irons in terms of high temperature use, is carried out and the effect of microstructural features on wear resistance is examined. The findings should be considered as preliminary data for the usability of new generation alloys as wear-resistant spheroidal graphite cast irons as alternatives to SiMo material in industrial platforms.

2. Materials and methods

All cast irons are produced by sand mold casting as Y blocks according to ASTM A536-84 standard. A laboratory scale induction furnace (Inductotherm, 35 kW) of 25 kg capacity is used for melting and casting is carried out from a temperature of 1560 °C. The chemical compositions of the cast irons are verified using an optical emission spectrometer (OES, Foundary Master) and the results are listed in Table 1.

Table 1: *Chemical compositions (wt.%) of the studied cast irons.*

Cast iron	C	Si	Mn	Mo	Nb	W
SiMo	3.51	4.15	0.40	0.86	-	-
SiNb	3.57	4.04	0.23	-	0.96	-
SiW	3.45	4.12	0.21	-	-	0.92

Samples are taken from the bulk materials, and their surfaces are etched with 3% nital after grinding and polishing. Then the solidification structures are characterized using a light microscope (LM, Olympus BX41M-LED) and quantitative analysis is carried out according to ISO 945–2, by an image analyzer (Leica Las V4.12) in order to determine the area % of graphite embedded in the solidified structure. Hardness is determined as the primary mechanical property of cast irons, and tests are carried out under 10 kgf load using a micro Vickers hardness tester (Emco-Test).

Cast irons and alumina ball as counterpart material are subjected to a tribological interaction for 150 m under dry friction conditions at a nominal load of 10 N and a ball sliding speed of 0,08 m/s. After dry friction tests, the change in the coefficient of friction for each cast iron is monitored as a function of sliding distance. Specific wear rates are calculated by determining the volume losses occurring during the tribological interaction in accordance with the ASTM G133-05 standard. The wear surfaces are characterized microscopically, and the dominant wear type for each cast iron in tribological interaction is examined.

3. Results and Discussion

Figure 1 shows the etched microstructures of the cast irons. Graphite (G), Mo-rich carbide and partial pearlite (P) phase regions are observed in the ferritic (F) matrix in the SiMo cast iron structure (Figure 1a). In the solidification structure of SiNb cast iron (Figure 1b), it is observed that graphite and pearlite exist in the ferritic matrix and that the matrix also contains Nb-rich carbide. Similar phase components are found in the solidification structure of SiW cast iron (Figure 1c), and it has been observed that W-rich carbides are dispersed in the ferritic matrix due to the presence of another carbide-forming element i.e. tungsten in the composition.

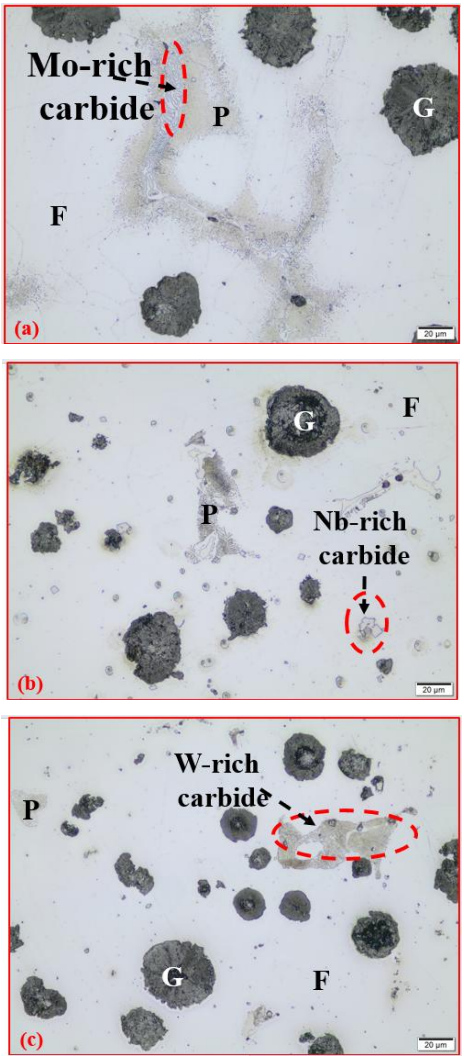

Fig. 1. *LM images showing the microstructural features within the cast irons; (a) SiMo, (b) SiNb and (c) SiW.*

The morphologies of the graphite found in the microstructure of such cast irons are affected by possible chemical composition changes and the morphological change can be monitored. Although no significant change is observed in the spherical morphology of graphite in cast iron matrices, a significant change is observed in the amount of graphite and image analysis studies reveal that the graphite content (area-%) in SiNb and SiW cast irons is 4.02 and 4.30, respectively, compared to SiMo cast iron (5.80). It is inevitable that the change in the type and amount of carbide, as well as the change in the amount of graphite in the ferritic matrix, will affect the mechanical properties. Thus, a significant change in the hardness of cast irons is also observed depending on the microstructural features; SiNb (228± 7 HV10) and SiW (218 ± 5 HV10) cast irons have higher hardness values compared to SiMo cast iron (192 ± 5 HV10).

CoF changes as a function of sliding distance in the tribological interactions of cast irons with a hard ceramic material are given in Figure 2. Among the cast irons tested, SiNb cast iron exhibits the highest coefficient of friction (0.040) over the total sliding distance. In tribological interaction, the amount of graphite in the matrix that can provide a lubricating effect can be a determining factor in the change of CoF values. In Figure 3, the effect of the amount of graphite in the matrix on the CoF values of each cast iron in the steady state is correlated and the findings indicate that CoF decreases as the graphite content increases.

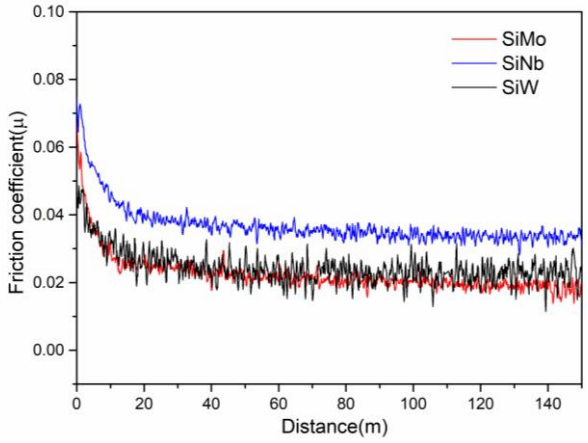

Fig. 2. *COF variation for cast irons as a function of sliding distance.*

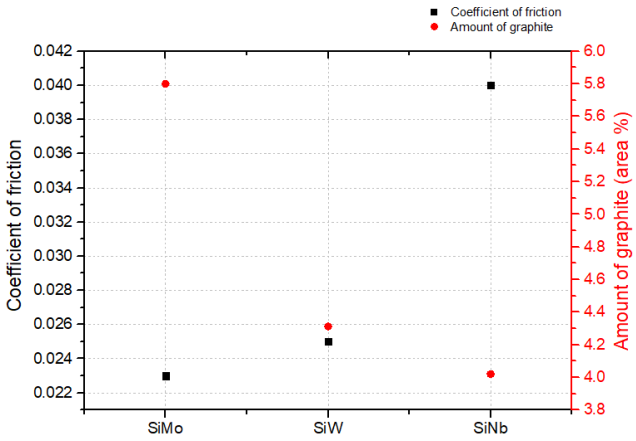

Fig. 3. *Relationship between CoF and graphite content values of the studied cast irons.*

In tribological interaction, hard phases like carbides that may be present in the matrix have a direct effect on material loss during wear. Primary Nb-rich carbides found in the solidification structure of SiNb cast iron are faceted hard phases that can crystallize directly from the liquid phase. These types of carbides can be harder than Mo-rich and W-rich carbides, which solidify from liquid by eutectic reaction. Although the pearlite phase with lamellar morphology in the ferritic matrix also contains carbide like cementite, primary and eutectic carbides, which have a coarse distribution within the solidified structure, are more decisive in the final hardness of the material. In Figure 4, the relationship between the hardness values of cast irons and the specific wear rates calculated after tribological tests is diagrammed. The findings indicate that there is a decrease in specific wear rates due to the

increase in material hardness. After tribological tests, LM examinations are carried out on the worn surfaces and the obtained micrographs are given in Figure 5. Worn surfaces typically indicate the presence of two tribological patterns along the sliding direction; (i) scratches due to abrasion and (ii) layers due to adhesion. Such patterns are mostly observed in ferritic matrix cast irons. It should be noted that abrasive wear occurs when the cast iron is scratched by a hard counterpart material and particles separated from the surface move as free bodies on the surface and may cause re-scratching. Although the surface roughness can be reduced under friction conditions, it is possible for cold metal to adhere to the surface due to adhesive wear. Adhesion causes a layer to form on the surface and it is also possible for the layers to undergo delamination and separate from the surface.

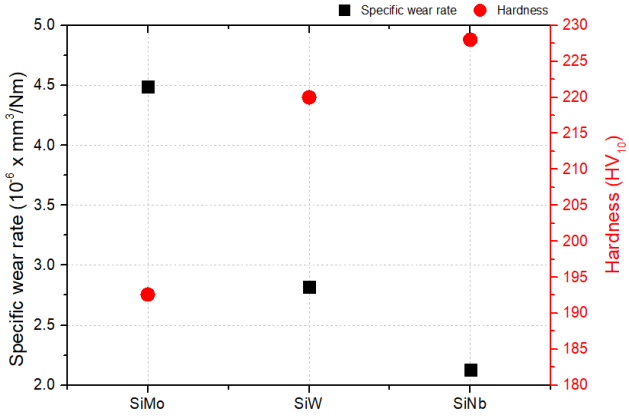

Fig. 4. *Relationship between specific wear rate and matrix hardness values of the studied cast irons.*

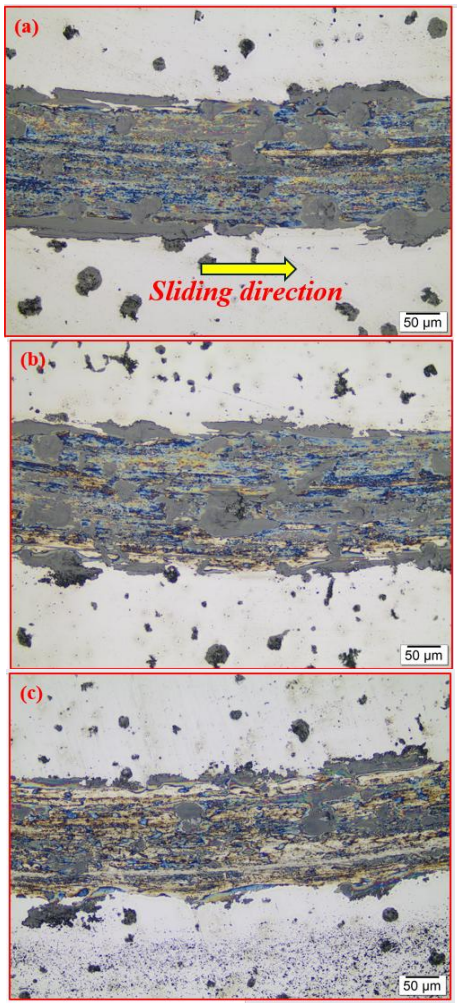

Fig. 5. *LM images showing the worn surfaces of the cast irons; (a) SiMo, (b) SiNb and (c) SiW.*

4. Conclusion

In this study, the tribological behavior of new generation cast irons (SiNb and SiW) developed as alternatives to cast irons containing high silicon and molybdenum (SiMo) is investigated under dry friction conditions. The findings reveal the presence of graphite phase with spheroidal morphology and pearlite phase in the ferritic matrix, together with carbides, with varying hardness and morphology, of the carbide-forming elements (i.e. Mo, Nb and W) in the chemical composition. Compared to SiMo cast iron, lower graphite amounts are detected in the solidification structure of new generation cast irons. A significant increase is observed in the CoF values of cast irons due to the decreasing amount of graphite under dry friction test conditions. Such a finding is evaluated as an indicator that high CoF values would be achieved if the lubricating effect of graphite decreases. However, the effect of matrix hardness on tribological interaction, especially on the specific wear rate, is observed quite clearly. Novel cast irons have higher hardness values and relatively lower specific wear rates compared to SiMo cast iron. Characterization studies on wear tracks indicate that adhesive wear is the dominant wear mechanism for all ductile cast irons due to the presence of their ferritic matrix.

Acknowledgements

The authors wish to acknowledge the financial support given by the Scientific Research Projects Coordination Unit of Kocaeli University under the project number *FUI-2024-3315* and TÜBİTAK 2209-B University Students Research Projects Support Program under the project number *1139B412303553*.

References

[1] Åberg, L.M., Hartung, C., *Trans. Indian Inst. Met.*, **65**, 633-636 (2012).
[2] Kazdal Zeytin, H., Kubilay, C., Aydin, H., Ebrinc, A.A., Aydemir, B., *J. Iron Steel Res. Int.*, **16**, 32-36 (2009).
[3] Lekakh, S.N., Tucker, W., Bofah, A., Selly, T., Godlewski, T., Li, M., *Oxid. Met.*, **94**, 251-264 (2020).
[4] Berggren, C., Magnusson, T., *Energy Policy*, **41**, 636-643 (2012).
[5] Agarwal, A.K., Mustafi, N.N., *Renew. Sustain. Energy Rev.*, **137**, 110624 (2021).
[6] Stawarz, M., Nuckowski, P.M., *Materials*, **15**(9), 3225 (2022).
[7] Aktaş Çelik, G., Polat, Ş., Atapek, Ş., Haidemenopoulos, G.N., *Bayburt Univ. Sci. J.*, **1**(1), 15-21 (2018).
[8] Sheikh, M.A., Iqbal, J., *J. Rare Earths*, **25**(5), 533-536 (2007).
[9] Fras, E., Gorny, M., *Arch. Metall. Mater.*, **57**(3), 767-777 (2012).
[10] Alonso, G., Ştefănescu, D.M., de La Fuente, E., Larrañaga, P., Suárez, R., *Mater. Sci. Forum*, **925**, 78-85 (2018).
[11] Stawarz, M., *Arch. Foundry Eng.*, **17**(1), 142-157 (2017).
[12] Alhussein, A., Risbet, M., Bastien, A., Chobaut, J.P., Balloy, D., Favergeon, J., *Mater. Sci. Eng. A*, **605**, 222-228 (2014).
[13] Aktaş Çelik, G., Atapek, Ş.H., Polat, Ş., Haidemenopoulos, G.N., *Metall. Mater. Trans. A*, **53**, 1991-2003 (2022).
[14] Ibrahim, M.M., Nofal, A., Mourad, M.M., *Metall. Mater. Trans. B*, **48**, 1149-1157 (2017).
[15] Abdelrahim, D.M., Ateia, E.E., Nofal, A.A., *Int. J. Metalcast.* (to be published).
[16] Delprete, C., Sesana, R., *Mater. Des.*, **57**, 528-537 (2014).
[17] Aktaş Çelik, G., Tzini, M.-I.T., Polat, Ş., Atapek, Ş.H., Haidemenopoulos, G.N., *Metall. Mater. Eng.*, **26**(1), 15-29 (2020).